

Well-Defined Alkyl Heteroscorpionate Magnesium Complexes as Excellent Initiators for the ROP of Cyclic Esters

Luis F. Sánchez-Barba,^{*,†} Andrés Garcés,[†] Mariano Fajardo,[†] Carlos Alonso-Moreno,[†]
 Juan Fernández-Baeza,^{*,‡} Antonio Otero,^{*,‡} Antonio Antiñolo,[‡] Juan Tejada,[‡]
 Agustín Lara-Sánchez,[‡] and María I. López-Solera[‡]

Departamento de Química Inorgánica y Analítica, Universidad Rey Juan Carlos, Móstoles-28933-Madrid, Spain, and Departamento de Química Inorgánica, Orgánica y Bioquímica, Universidad de Castilla-La Mancha, Campus Universitario, 13071-Ciudad Real, Spain

Received July 20, 2007

The reaction of the heteroscorpionate lithium salts [Li(tpamd)(THF)] [tpamd = *N*-ethyl-*N'*-*tert*-butylbis(3,5-dimethylpyrazol-1-yl)acetamidinate] and [Li(pbpamd)(THF)] [pbpamd = *N,N'*-diisopropylbis(3,5-dimethylpyrazol-1-yl)acetamidinate] with 1 equiv of RMgCl proceeds to give very high yields of the neutral heteroscorpionate alkyl magnesium complexes [Mg(R)(NNN)] (NNN = tpamd, R = C₃H₅ **1**, ^tBu **2**, CH₂SiMe₃ **3**; NNN = pbpamd, R = C₃H₅ **4**, ^tBu **5**, CH₂SiMe₃ **6**). On heating toluene solutions of complexes **1–3**, **5**, and **6**, a ligand redistribution process occurs to give the corresponding 6-coordinated sandwich complexes [Mg(tpamd)₂] (**7**) and [Mg(pbpamd)₂] (**8**). Interestingly, the allyl derivative **4** can be easily transformed to **8** at room temperature. In addition, the cationic sandwich complex [Mg(tpamdH)₂]-Cl₂ (**9**) [tpamdH = *N*-ethyl-*N'*-*tert*-butylbis(3,5-dimethylpyrazol-1-yl)acetamidine] was obtained from **7** by means of a protonation process. Finally, alkyl-containing complexes **1–6** can act as highly effective single-component living initiators for the ring-opening polymerization of ϵ -caprolactone and lactides over a wide range of temperatures. ϵ -Caprolactone is polymerized within seconds to give high molecular weight polymers with narrow polydispersities. Lactide afforded PLA materials with medium molecular weights and polydispersities as narrow as $M_w/M_n = 1.05$. Additionally, polymerization of L-lactide occurred without racemization in the propagation process and offered highly crystalline, isotactic poly(L-lactides) with high melting temperatures ($T_m = 160$ °C). Polymer end-group analysis shows that the polymerization process is initiated by alkyl transfer to the monomer.

Introduction

Polymerization of cyclic esters such as ϵ -caprolactone and lactides has been reported extensively in the literature for various single-site metal catalysts.^{1,2} Lactide, the cyclic dimer of lactic acid, is an inexpensive and renewable natural feedstock³ that is a byproduct of biomass fermentation. The biocompatible nature of this compound with living tissues and the nontoxic nature of polylactides (PLAs), which also constitute an important emerging class of environmentally friendly and biodegradable thermoplastics, has enhanced the study of these materials in biomedical applications, for example, in resorbable sutures,^{4,5}

drug delivery agents,⁵ and artificial matrix tissues.⁶ These medicinal applications have promoted the use of biocompatible metals. Trace amounts of the catalyst may be tenaciously incorporated within the polymer, and, as with any polymer that is of commercial interest in the biomedical field, it is important that the metal be biologically benign and that any residual catalyst does not impart undesirable properties such as color to an otherwise colorless polymer. In this regard, magnesium is an attractive metal. Magnesium is an essential nutrient and mineral for plants and humans.⁷ Zinc, calcium, and to a lesser extent magnesium complexes with sterically hindered ligands have been shown to be the most efficient initiators to date for the well-controlled ring-opening polymerization of the aforementioned polar monomers.^{1,2} Coates and Chisholm independently reported diketimato and iminophenolato complexes of zinc that are very efficient for the polymerization of lactides.⁸ Chisholm also found that tris(pyrazolyl)hydroborate complexes

* Corresponding authors. E-mail: luisfernando.sanchezbarba@urjc.es (L.F.S.-B.); juan.fbaeza@uclm.es (J.F.-B.); a.otero@uclm.es (A.O.).

[†] Universidad Rey Juan Carlos.

[‡] Universidad de Castilla-La Mancha.

(1) (a) O'Keefe, B. J.; Hillmyer, M. A.; Tolman, W. B. *J. Chem. Soc., Dalton Trans.* **2001**, 2215. (b) Coates, G. W. *J. Chem. Soc., Dalton Trans.* **2002**, 467.

(2) (a) Dechy-Cabaret, O.; Martin-Vaca, B.; Bourissou, D. *Chem. Rev.* **2004**, *104*, 6147. (b) Wu, J.; Yu, T.-L.; Chen, C.-T.; Lin, C.-C. *Coord. Chem. Rev.* **2006**, *250*, 602. (c) Chisholm, M. H.; Zhou, Z. *J. Mater. Chem.* **2004**, *14*, 3081.

(3) Biela, T.; Kowalski, A.; Libiszowski, J.; Duda, A.; Penczek, S. *Macromol. Symp.* **2006**, *47*.

(4) (a) Schmitt, E. E.; Polistina, R. A. U.S. Patent 3,463,158, 1969. (b) Frazza, E. J.; Schmitt, E. E. *J. Biomed. Mater. Res. Symp.* **1971**, *1*, 43. (c) Dexon and Vicryl are products of Davis & Geek Corp., Wayne, NJ, and Ethicon, Inc., Somerville, NJ, respectively.

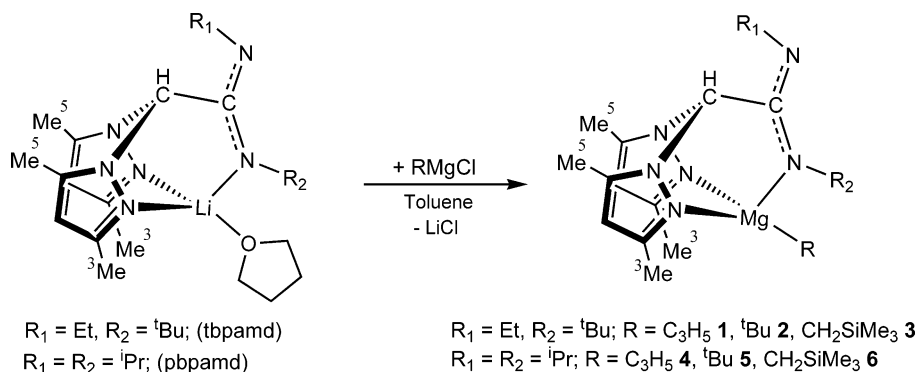
(5) (a) Leupron Depot is a product of Takeda Chemical Industries, Ltd., Japan, for drug delivery purposes. (b) Taehan Hwakakhoe *Chi* **34**, 203. *Chem. Abstr.* **1990**, *113*, 98014g.

(6) (a) Hubbell, J. A.; Langer, R. *Chem. Eng. News* **1995**, *Mar 13*, 42. (b) Langer, R.; Vacanti, J. P. *Science* **1993**, *260*, 920. (c) Chisholm, M. H.; Iyer, S. S.; McCollum, D. G.; Pagel, M.; Werner-Zwanziger, U. *Macromolecules* **1999**, *32*, 963.

(7) (a) Campbell, N. A. *Biology*, 3rd ed.; Benjamin/Cummings Publishing Co.: Redwood City, CA, 1993; pp 718 and 811. (b) Cowan, J. A., Ed. *The Biological Chemistry of Magnesium*; VCH: New York, 1995.

(8) (a) Chen, M.; Attygalle, A. B.; Lobkovsky, E. B.; Coates, G. W. *J. Am. Chem. Soc.* **1999**, *121*, 11583. (b) Chamberlain, B. M.; Cheng, M.; Moore, D. R.; Ovitt, E. B.; Lobkovsky, E. B.; Coates, G. W. *J. Am. Chem. Soc.* **2001**, *123*, 3229. (c) Chisholm, M. H.; Galluci, J.; Zhen, H.; Huffman, J. C. *Inorg. Chem.* **2001**, *40*, 5051. (d) Chisholm, M. H.; Galluci, J.; Phomphrai, K. *Inorg. Chem.* **2002**, *41*, 2785.

Scheme 1. Synthesis of the Heteroscorpionate Alkyl Magnesium Complexes 1–6



of magnesium and especially calcium were highly active,⁹ showing high levels of stereocontrol in the polymer microstructures as well as narrow molecular weight distributions.

During the past decade, our research group has contributed widely to the design of new “heteroscorpionate” ligands¹⁰ related to the bis(pyrazol-1-yl)methane system,¹¹ with several pendant donor arms such as carboxylate,¹² dithiocarboxylate,¹³ methoxy,¹⁴ cyclopentadienyl,¹⁵ acetaminate and thioacetaminate groups,¹⁶ and, more recently, amidinate¹⁷ groups. It is well known that heteroscorpionate ligands have proved to be excellent ancillary ligands for the synthesis of a variety of organometallic early transition metal complexes.^{11–17} We have now turned our attention to the exploration of the reactivity of the recently reported amidinate-based heteroscorpionate ligands¹⁷ as convenient ancillary ligands for the synthesis of alkyl-containing magnesium complexes.

The work described here concerns our initial approach to the preparation of a new class of organomagnesium complexes of the type $[\text{Mg}(\text{R})(\text{NNN})]$, where NNN are amidinate-based heteroscorpionates. The interesting temperature-dependent behavior of these compounds and their reactivity as single-component living initiators for the well-controlled ring-opening polymerization of ϵ -caprolactone and *L*-*rac*-lactide are also described.

Results and Discussion

Synthesis and Characterization of Complexes. Cooled ($-70\text{ }^\circ\text{C}$) toluene solutions of the heteroscorpionate lithium salts $[\text{Li}(\text{tbpamd})(\text{THF})]^{17}$ [tbpamd = *N*-ethyl-*N'*-*tert*-butylbis(3,5-dimethylpyrazol-1-yl)acetamidinate] and $[\text{Li}(\text{pbpamd})(\text{THF})]^{17}$ [pbpamd = *N,N'*-diisopropylbis(3,5-dimethylpyrazol-1-yl)acetamidinate] were treated with a series of Grignard reagents RMgCl ($R = \text{C}_3\text{H}_5, \text{}^t\text{Bu}, \text{CH}_2\text{SiMe}_3$) in a 1:1 molar ratio. These reactions gave rise to heteroscorpionate alkyl magnesium complexes $[\text{Mg}(\text{R})(\text{NNN})]$ (NNN = tbpamd, $R = \text{C}_3\text{H}_5$ **1**, ^tBu **2**, CH_2SiMe_3 **3**; NNN = pbpamd, $R = \text{C}_3\text{H}_5$ **4**, ^tBu **5**, CH_2SiMe_3 **6**) as yellow or orange solids in good yields (ca. 80%) after the appropriate workup (see Scheme 1). The compounds are extremely air and moisture sensitive, and are highly soluble in THF or toluene and sparingly soluble in *n*-hexane or diethyl ether, apart from derivatives **3** and **6**, which are soluble in these solvents. All of the compounds decompose in dichloromethane. Magnesium mono-alkyl complexes supported by different tris(pyrazolyl)hydroborate ligands have been reported previously,^{9,18} but these compounds were obtained by a metathetical reaction between MgR_2 and potassium/thallium(I) tris(pyrazolyl)hydroborate or tris(indazolyl)hydroborate to avoid the competition between alkyl and halide bond metathesis in the direct reaction with RMgX . However, the monoalkyl complexes **1–6** were easily obtained at room temperature by reaction with RMgX . Qualitative tests showed the absence of halide through the formation of $[\text{MgX}(\text{NNN})]$ derivatives.

The ^1H and $^{13}\text{C}\{^1\text{H}\}$ NMR spectra of **1–6** each show a simple set of resonances for the pyrazole rings, indicating that both pyrazole rings are equivalent. These data suggest a tetrahedral disposition for the magnesium atom with κ^3 -NNN-coordination of the heteroscorpionate ligand, a situation in which a plane of symmetry exists and contains the amidinate group and the alkyl ligand (Scheme 1). The NMR signals due to the amidinate moiety of the magnesium compounds **4–6** (where $R_1 = R_2$) show two sets of resonances for these substituents. This observation is indicative of a monodentate binding of the amidinate moiety to the magnesium atom. Additionally, a doublet for protons H_{anti} and H_{syn} , and a multiplet for the central proton $\text{H}_{\text{methine}}$, indicate σ - π fluxional behavior of the allyl ligand in solution for **1** and **4**. The $^{13}\text{C}\{^1\text{H}\}$ NMR spectra of these complexes at $20\text{ }^\circ\text{C}$ are also consistent with the presence of a fluxional allyl ligand. ^1H NOESY-1D experiments were

(9) (a) Chisholm, M. H.; Eilerts, N. W. *Chem. Commun.* **1996**, 853. (b) Chisholm, M. H.; Eilerts, N. W.; Huffman, J. C.; Iyer, S. S.; Pacold, V.; Phomphrai, K. *J. Am. Chem. Soc.* **2000**, *122*, 11845. (c) Chisholm, M. H.; Galluci, J.; Phomphrai, K. *Chem. Commun.* **2003**, 48.

(10) Trofimenko, S. *Scorpionates. The Coordination Chemistry of Polypyrazolylborate Ligands*; Imperial College Press: London, 1999.

(11) (a) Otero, A.; Fernández-Baeza, J.; Antiñolo, A.; Tejada, J.; Lara-Sánchez, A. *Dalton Trans.* **2004**, 1499. (b) Pettinari, C.; Pettinari, R. *Coord. Chem. Rev.* **2005**, *249*, 663.

(12) A representative example: Otero, A.; Fernández-Baeza, J.; Antiñolo, A.; Tejada, J.; Lara-Sánchez, A.; Sánchez-Barba, L.; Martínez-Caballero, E.; Rodríguez, A. M.; López-Solera, I. *Inorg. Chem.* **2005**, *44*, 5336.

(13) A representative example: Otero, A.; Fernández-Baeza, J.; Antiñolo, A.; Carrillo-Hermosilla, F.; Tejada, J.; Lara-Sánchez, A.; Sánchez-Barba, L.; Fernández-López, M.; López-Solera, I. *Inorg. Chem.* **2004**, *43*, 1350.

(14) Otero, A.; Fernández-Baeza, J.; Antiñolo, A.; Tejada, J.; Lara-Sánchez, A.; Sánchez-Barba, L.; Rodríguez, A. M. *Eur. J. Inorg. Chem.* **2004**, 260.

(15) Otero, A.; Fernández-Baeza, J.; Antiñolo, A.; Tejada, J.; Lara-Sánchez, A.; Sánchez-Barba, L.; Rodríguez, A. M.; Maestro, M. A. *J. Am. Chem. Soc.* **2004**, *126*, 1330.

(16) (a) Otero, A.; Fernández-Baeza, J.; Antiñolo, A.; Tejada, J.; Lara-Sánchez, A.; Sánchez-Barba, L.; Sánchez-Molina, M.; Franco, S.; López-Solera, I.; Rodríguez, A. M. *Eur. J. Inorg. Chem.* **2006**, 707. (b) Otero, A.; Fernández-Baeza, J.; Antiñolo, A.; Tejada, J.; Lara-Sánchez, A.; Sánchez-Barba, L.; Sánchez-Molina, M.; Franco, S.; López-Solera, I.; Rodríguez, A. M. *Dalton Trans.* **2006**, 4359.

(17) Otero, A.; Fernández-Baeza, J.; Antiñolo, A.; Tejada, J.; Lara-Sánchez, A.; Sánchez-Barba, L.; López-Solera, I.; Rodríguez, A. M. *Inorg. Chem.* **2007**, *46*, 1760.

(18) (a) Han, R.; Looney, A.; Parkin, G. *J. Am. Chem. Soc.* **1989**, *111*, 7276. (b) Han, R.; Parkin, G. *J. Am. Chem. Soc.* **1990**, *112*, 3662. (c) Han, R.; Brachrach, M.; Parkin, G. *Polyhedron* **1990**, *9*, 1775. (d) Han, R.; Parkin, G. *Organometallics* **1991**, *10*, 1010. (e) Han, R.; Parkin, G. *J. Am. Chem. Soc.* **1992**, *114*, 748. (f) Kisko, J.-L.; Fillebeen, T.; Hascall, T.; Parkin, G. *J. Organomet. Chem.* **2000**, *596*, 22.

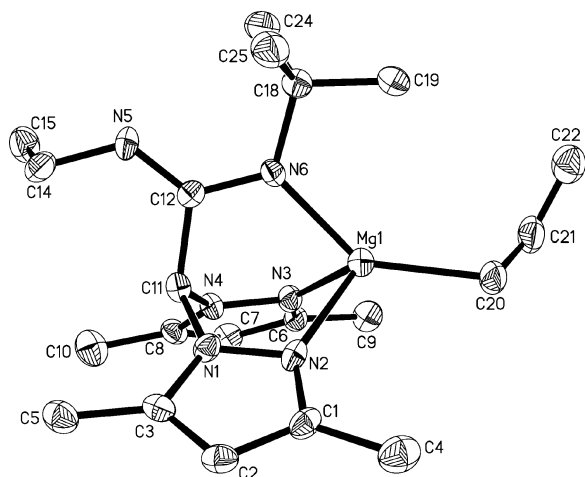


Figure 1. ORTEP view of $[\text{Mg}(\text{C}_3\text{H}_5)(\text{tbpamd})]$ (**1**). Hydrogen atoms have been omitted for clarity. Thermal ellipsoids are drawn at the 50% probability level.

Table 1. Selected Interatomic Distances (Å) and Angles (deg) for **1** and **9**

1		9	
Mg(1)–N(2)	2.126(3)	Mg(1)–N(1)	2.21(1)
Mg(1)–N(3)	2.122(3)	Mg(1)–N(3)	2.18(1)
Mg(1)–N(6)	2.050(3)	Mg(1)–N(6)	2.15(1)
Mg(1)–C(20)	2.133(4)	N(5)–C(1)	1.36(2)
N(5)–C(12)	1.296(5)	N(6)–C(1)	1.28(2)
N(6)–C(12)	1.350(5)	C(1)–C(2)	1.54(2)
C(20)–C(21)	1.454(6)		
C(21)–C(22)	1.328(6)		
N(2)–Mg(1)–N(3)	86.8(1)	N(1)–Mg(1)–N(3)	85.6(6)
N(2)–Mg(1)–N(6)	90.7(1)	N(1)–Mg(1)–N(6)	82.9(6)
N(3)–Mg(1)–N(6)	89.6(1)	N(3)–Mg(1)–N(6)	82.9(6)
N(6)–Mg(1)–C(20)	138.8(2)	N(6)–Mg(1)–N(6) ^a	180.0(1)
C(12)–N(6)–C(18)	119.4(3)	N(5)–C(1)–N(6)	125(1)
N(5)–C(12)–N(6)	125.8(3)	N(5)–C(1)–C(2)	118(2)
Mg(1)–C(20)–C(21)	115.4(3)	C(1)–N(5)–C(13)	139(2)
C(20)–C(21)–C(22)	128.5(4)		

^a Symmetry transformation used to generate equivalent atom: $-x + 1, -y, -z$.

also performed to confirm the assignment of the signals for the Me^3 , Me^5 , and H^4 groups of the pyrazole rings. Furthermore, in the case of compounds **1–3** (where $\text{R}_1 \neq \text{R}_2$), the response in the ^1H NOESY-1D experiment from the Me^5 protons of the pyrazole rings on irradiation of the ethyl group of the amidinate moiety suggests that this group is located in the R_1 position, whereas the *tert*-butyl group is in the R_2 position (Scheme 1).

Single crystals of **1** suitable for X-ray diffraction crystallography were readily grown from toluene at $-26\text{ }^\circ\text{C}$. The ORTEP representation of complex **1** is shown in Figure 1. Selected bond lengths and angles are collected in Table 1. The magnesium center exhibits a distorted tetrahedral geometry, in which the pyrazolic nitrogens N(2) and N(3) occupy two positions, and the amidinate nitrogen N(6) and the η^1 -allyl group the other two positions. The distortion is due to the heteroscorpionate ligand, which acts in a κ^3 -NNN coordination mode. The N(2)–Mg and N(3)–Mg bond lengths [2.126(3) and 2.122(3) Å] (Table 1) are very similar and are comparable to that observed in the lithium salt.¹⁷ The four-membered Mg–N(6)–C(12)–C(11) fragment and the allyl group are contained in a symmetric plane of the molecule. The solid-state structure also confirms that the amidinate moiety is coordinated in a monodentate fashion to the Mg atom, and this behavior is relatively

unusual.^{17,19} The N(6)–Mg bond length [2.050(3) Å] is shorter than the N(2)–Mg and N(3)–Mg ones but longer than that in the lithium salt [1.983(1) Å].¹⁷ The delocalization is clear in the N–C–N core, with C(12)–N(6) = 1.350(5) Å and C(12)–N(5) = 1.296(5) Å. Finally, the allyl fragment is η^1 -bonded in the solid state with two different bond lengths, C(20)–C(21) = 1.454(6) Å for the single bond and C(21)–C(22) = 1.328(6) Å for the double bond. Whereas the C(20) carbon shows essentially sp^3 hybridization, as demonstrated by the Mg–C(20)–C(21) angle of $115.4(3)^\circ$, the C–C–C angle around the sp^2 carbon C(21) is widened to $128.5(4)^\circ$.

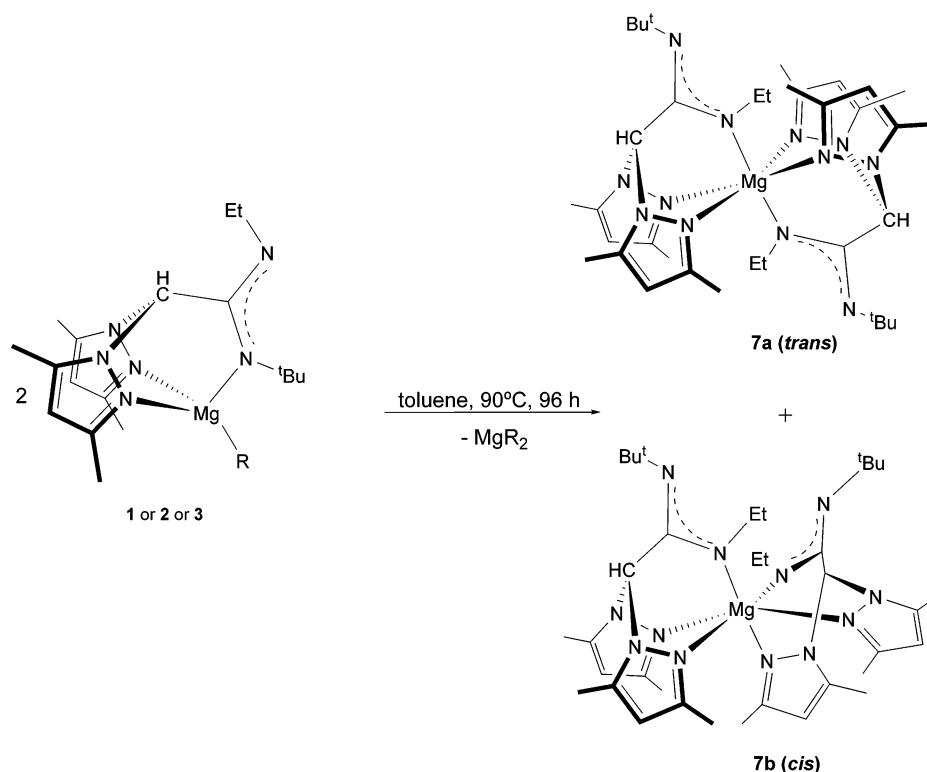
In view of the well-known fact that Grignard reagents exist in solution as a complex mixture of species due to the facile ligand redistribution reactions, for example, the Schlenk equilibrium,²⁰ we investigated the possibility of similar ligand redistribution reactions for the heteroscorpionate alkyl magnesium complexes synthesized $[\text{Mg}(\text{R})(\text{NNN})]$ **1–6**, a type of behavior previously observed in similar homoscorpionate alkyl magnesium systems.¹⁸ We observed that solutions of derivatives **1–3**, **5**, and **6** are stable at room temperature during days, while heating toluene solutions at $90\text{ }^\circ\text{C}$ for 96 h resulted in a ligand redistribution process that led to the formation of the corresponding 6-coordinated sandwich complexes $[\text{Mg}(\text{tbpamd})_2]$ (**7**) (Scheme 2) and $[\text{Mg}(\text{pbpamd})_2]$ (**8**) (Scheme 3). Interestingly, the allyl derivative **4** can be easily transformed into the sandwich complex **8** at room temperature after 2 h (Scheme 3). These ligand-exchange processes are undoubtedly a consequence of the low steric demand of the methyl groups from the bis(3,5-dimethylpyrazol-1-yl)methane fragment, which are not sufficiently bulky to behave as “tetrahedral enforcer” units, as found when *t*Bu substituents are present in the pyrazole rings.¹⁸

The ^1H and $^{13}\text{C}\{^1\text{H}\}$ NMR spectra of **7** in benzene-*d*₆ at room temperature reveal the presence of the two possible isomers in an equal ratio in solution. The less congested (*trans*) isomer **7a** has both amidinate fragments in mutually *trans* positions, and this displays one set of signals for the H^4 , Me^3 , Me^5 , CH protons, and for the amidinate fragments, thus showing a symmetric arrangement in solution. The most congested (*cis*) isomer **7b** has the two amidinate fragments in mutually *cis* positions and presents two sets of resonances for H^4 , Me^3 , and Me^5 and two sets for the amidinate fragments, thus indicating that the pyrazole rings are inequivalent in each of the heteroscorpionate ligands. In the sandwich complex, both ligands are equivalent. In the sandwich complex **7**, the response in the ^1H NOESY-1D experiment from the Me^5 protons of the pyrazole rings on irradiation of the *tert*-butyl group of the amidinate moiety suggests that this group is on the nitrogen bonded to the methine group, whereas the ethyl group is orientated toward the metal, probably to generate a less congested arrangement in the sandwich complex (Scheme 2). Surprisingly, compound **8** displays two sets of resonances for H^4 , Me^3 , and Me^5 and two sets for the amidinate groups, an observation in good agreement with the exclusive presence of the most congested *cis* isomer.

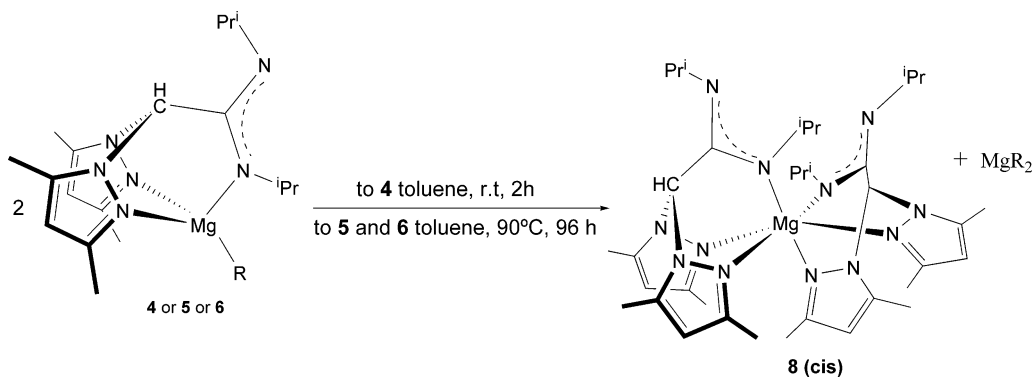
(19) (a) Grove, D. M.; van Koten, G.; Ubbels, H. J. C.; Vrieze, K.; Niemann, L. C.; Stam, C. H. *J. Chem. Soc., Dalton Trans.* **1986**, 717. (b) Zinn, A.; Dehnicke, L.; Fenske, D.; Baum, G. *Z. Anorg. Allg. Chem.* **1991**, 596, 47. (c) Foley, S. R.; Bensimon, C.; Richeson, D. S. *J. Am. Chem. Soc.* **1997**, 119, 10359.

(20) The simple model of the Schlenk equilibrium ($2\text{RMgX} \rightleftharpoons \text{MgR}_2 + \text{MgX}_2$) for describing the composition of Grignard reagents is complicated by a variety of factors including (i) the formation of complexes of each component with either solvent, reactant, or product, (ii) the formation of dimeric (or higher order) species, and (iii) the presence of ionic species. (a) Kharasch, M. S.; Reinmuth, O. *Grignard Reactions of Nonmetallic Substances*; Prentice Hall: New York, 1954. (b) Ashby, E. C. *Pure Appl. Chem.* **1980**, 52, 545. (c) Ashby, E. C. *Q. Rev.* **1967**, 259. (d) Ashby, E. C.; Laemmle, J.; Neumann, H. M. *Acc. Chem. Res.* **1974**, 7, 272.

Scheme 2. Synthesis of the Heteroscorpionate Sandwich Complex 7



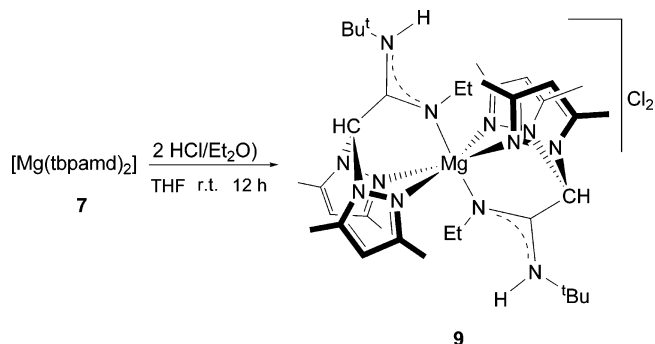
Scheme 3. Synthesis of the Heteroscorpionate Sandwich Complex 8



This indicates that in this sandwich disposition $[\text{Mg}(\text{NNN})_2]$ the most congested cis isomer is probably the most thermodynamically stable.

Finally, a protonation reaction process was observed when we attempted different procedures to obtain single crystals suitable for X-ray diffraction from solutions of complex 7. For example, when a CDCl_3 solution of 7 was slowly evaporated at room temperature in an air atmosphere, after 72 h yellow crystals were deposited from the solution, and these were identified as the cationic sandwich complex $[\text{Mg}(\text{tbpamdH})_2]\text{Cl}_2$ (9) [tbpamdH = *N*-ethyl-*N'*-*tert*-butylbis(3,5-dimethylpyrazol-1-yl)acetamidine]. The presence of adventitious HCl, arising from CDCl_3 in the reaction mixture during the crystallization process, was probably responsible for the protonation of both acetamidate moieties of the heteroscorpionate ligands and their transformations into acetamidine units. This type of process has been observed in other heteroscorpionate ligands prepared in our research group. For example, we recently published¹⁶ the transformation by protonation of acetamidate and thioacetamidate moieties into acetamide or thioacetamide units, respectively. Additionally, we directly prepared complex 9 by addition of

Scheme 4. Synthesis of the Cationic Sandwich Complex 9



the appropriate amount of HCl in diethyl ether to a solution of complex 7 in THF (Scheme 4).

The ^1H and $^{13}\text{C}\{^1\text{H}\}$ NMR spectra of 9 show one set of resonances for the two acetamidine moieties of the heteroscorpionate ligands. In addition, the ^1H NMR spectrum of this complex exhibits a singlet at 7.71 ppm, which corresponds to the N–H group of both acetamidine moieties. The X-ray molecular structure of 9 has been established (Figure 2). The

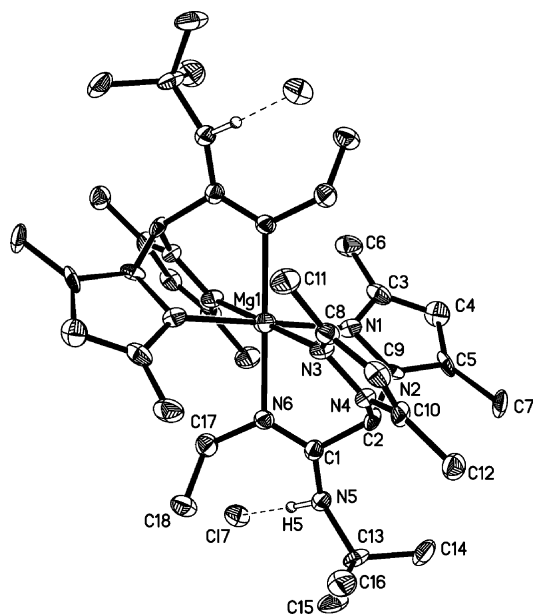


Figure 2. ORTEP view of $[\text{Mg}(\text{tpamdH})_2]\text{Cl}_2$ (**9**). Thermal ellipsoids are drawn at the 30% probability level. Hydrogen atoms have been omitted for clarity, except H5 [C17...H5 2.40(12), C17...N5 3.36(1), C17...H5-N5 1.69(9)].

cationic complex shows two heteroscorpionate ligands symmetrically coordinated to the magnesium atom in a κ^3 -NNN mode. In its structure, the magnesium atom exhibits an octahedral geometry, with the pyrazolic nitrogens N(1) and N(3) in the equatorial plane, and the acetamidine nitrogen N(6) in the axial position [N(1)–Mg(1)–N(3) and N(6)–Mg(1)–N(6a) of 85.6(6)° and 180.0(1)°, respectively]. N(1)–Mg(1), N(3)–Mg(1), and N(6)–Mg bond distances of 2.21(1), 2.18(1), and 2.15(1) Å, respectively, are longer than that observed in the monoalkyl complex **1** (Table 1). N(5) is protonated and hydrogen bonded to Cl(7). Two chloroform deuterated disordered molecules are stabilizing the crystal by hydrogen-bond interactions.

Polymerization Studies. Complexes **1–6** were tested in the ring-opening polymerization of ϵ -caprolactone (CL) and L-/rac-lactide (L-LA, rac-LA). Alkyl initiators **1–6** act as highly active single-component catalysts for the polymerization of ϵ -caprolactone (CL) to give high molecular weight polymers; the results are collected in Table 2. A variety of polymerization conditions were explored. Complexes **1** and **2** initiate very rapid polymerization of CL at room temperature (entries 1 and 2), and **2** gives complete conversion of 500 equiv of CL in 15 min, with a productivity of more than 2×10^5 g PCL (mol Mg) $^{-1}$ h $^{-1}$. The polymerization is well controlled and gives high polymer molecular weights with a narrow polydispersity, suggestive of a living behavior ($M_w = 47\,000$, $M_w/M_n = 1.27$ for **2**). Complex **3** showed a very high activity, and, in 1 min, 97% of the polymer was recovered at room temperature with a productivity of more than 30×10^5 g PCL (mol Mg) $^{-1}$ h $^{-1}$ (entry 3). Complexes **4** and **5** gave higher productivity at room temperature than the equivalent alkyls **1** and **2** (entries 5 and 7), and **5** gave complete conversion of 500 equiv of CL in 10 min, with a productivity of more than 3×10^5 g PCL (mol Mg) $^{-1}$ h $^{-1}$. The productivity and molecular weight decreased markedly on cooling (entries 6 and 8), and at -20 °C only 10% of the polymer was recovered for **5**, with very narrow polydispersity ($M_w/M_n = 1.12$, entry 8), whereas **4** dramatically reduces the catalytic activity and only traces are found (entry 6). Additionally, derivative **6** proved to be an extremely active catalyst, with a productivity of more than 200×10^5 g PCL (mol Mg) $^{-1}$ h $^{-1}$ at room temperature

(entry 9). Furthermore, this activity was maintained at -60 °C (entry 10), and in 30 s 62% of the monomer was converted with a polydispersity value $M_w/M_n = 1.12$.

In these tests, the polymer molecular weights were limited by the monomer/initiator ratio of 500:1. An increase in this ratio by a factor of 10 gave polymers with significantly higher molecular weights ($M_w > 10^5$) and broader molecular weight distributions (entries 4 and 11), possibly due to the presence of back-biting as well as transesterification reactions.

In accordance with the aforementioned data, it is worth noting that the polymerization processes initiated by complexes **1–3** are significantly slower than those initiated by their counterparts **4–6**. This marked difference between the two types of derivatives is presumably a consequence of the sterically demanding environment created by the presence of the 'Bu group from the amidinate fragment in complexes **1–3**, a characteristic that may disfavor coordination of the monomer during the propagation step. Very few alkyl magnesium initiators^{21,22} have been shown to polymerize ϵ -caprolactone. Furthermore, to the best of our knowledge, examples of ROP processes for this monomer initiated by alkyl magnesium complexes have not been described previously²¹ with such good activity at very low temperatures (entry 10). End-group analysis showed that the polymers obtained with the initiators **3** and **6** contain $-\text{CH}_2\text{SiMe}_3$ termini, which provides evidence to confirm that the polymerization follows a nucleophilic route and is initiated by the transfer of an alkyl ligand to the monomer, with cleavage of the acyl–oxygen bond and formation of a metal alkoxide-propagating species.^{22,23} In general, the nature of the alkyl group in our initiators affects the catalytic activity, which under the present polymerization conditions decreases in the order $\text{CH}_2\text{SiMe}_3 \gg \text{'Bu} > \text{C}_3\text{H}_5$; this trend is consistent with the decrease in the lability of the M–C bond.²⁴

Derivatives **3** and **6** were also examined for the production of poly(lactides) (PLAs) (Table 3). Complex **6** proved to be an active catalyst for the polymerization of L-lactide at 70 °C in toluene (Table 3, entries 1–5). In all cases, the PLAs produced have molecular weights in close agreement with calculated values [$M_n(\text{calcd})\text{PLA}_{100} = 14\,400$] (Table 3). At this point, it is worth mentioning that polymerization of the optically active (*S,S*)-lactide (L-lactide) afforded 93% conversion of 100 equiv in 96 h, with a very narrow molecular weight distribution ($M_w/M_n = 1.19$, entry 4). The polymerization occurs without epimerization reactions and affords highly crystalline, isotactic polymers with a T_m in the range of 155–160 °C.²⁵ The low level of stereochemical imperfections is also revealed in the poly(L-lactide) with $M_w > 10\,000$, where the optical activity remains almost constant, $[\alpha]^{22}_D = 146\text{--}147^\circ$. When the polymerization is carried out under bulk conditions, 70% of the polymer is recovered after 75 min, and the product has a broader polydispersity ($M_w/M_n = 1.40$, entry 5).

The high level of control afforded by this initiator in the polymerization of L-lactide is further exemplified by the narrow

(21) (a) Sarazin, Y.; Schormann, M.; Bochmann, M. *Organometallics* **2004**, *23*, 3296. (b) Sarazin, Y.; Howard, R. H.; Hughes, D. L.; Humphrey, S. M.; Bochmann, M. *Dalton Trans.* **2006**, 340.

(22) Sánchez-Barba, L. F.; Hughes, D. L.; Humphrey, S. M.; Bochmann, M. *Organometallics* **2006**, *25*, 1012.

(23) (a) Sánchez-Barba, L. F.; Hughes, D. L.; Humphrey, S. M.; Bochmann, M. *Organometallics* **2005**, *24*, 3792. (b) Sánchez-Barba, L. F.; Hughes, D. L.; Humphrey, S. M.; Bochmann, M. *Organometallics* **2005**, *24*, 5329.

(24) Martinho, J. A.; Beauchamp, J. L. *Chem. Rev.* **1990**, *90*, 629.

(25) (a) Radano, C. P.; Baker, G. L.; Smith, M. R. *J. Am. Chem. Soc.* **2000**, *122*, 1552. (b) Zhong, Z.; Dijkstra, J. P.; Feijen, J. *J. Am. Chem. Soc.* **2003**, *125*, 11291.

Table 2. Polymerization of ϵ -Caprolactone Catalyzed by Complexes 1–6^a

entry	initiator	[ϵ -CL] ₀ /[initiator] ₀	temp (°C)	time (min)	yield (g)	conv (%) ^b	prod ^c	<i>M</i> _w (Da) ^d	<i>M</i> _w / <i>M</i> _n ^d
1	1	500	20	15	4.32	84	192	34 000	1.16
2	2	500	20	15	4.95	96	220	47 000	1.27
3	3	500	20	1	4.98	97	3320	52 000	1.41
4	3^e	5000	20	5	6.53	57	3918	112 000	1.43
5	4	500	20	10	4.41	86	294	38 000	1.21
6	4	500	−20	10	traces				
7	5	500	20	10	4.97	97	331	51 000	1.33
8	5	500	−20	10	0.51	10	34	24 000	1.12
9	6	500	20	0.16	5.02	98	20 916	59 000	1.45
10	6	500	−60	0.5	3.18	62	4240	18 000	1.12
11	6^e	5000	20	5	9.69	87	5814	161 000	1.42

^a Polymerization conditions: 90 μ mol of initiator. ^b Percentage conversion of the monomer (weight monomer/weight of polymer recovered \times 100). ^c kg polymer \cdot (mol Mg)^{−1} h^{−1}. ^d Determined by GPC relative to polystyrene standards in tetrahydrofuran. ^e 20 μ mol of initiator.

Table 3. Polymerization of L-Lactide and *rac*-Lactide Catalyzed by Complexes 3 and 6^a

entry	initiator	monomer	temp (°C)	time (h)	yield (g)	conv (%) ^b	<i>M</i> _{n(theor.)} (Da) ^c	<i>M</i> _n (Da) ^d	<i>M</i> _w (Da) ^d	<i>M</i> _w / <i>M</i> _n ^d	<i>T</i> _m (°C) ^e	[α] _D ²⁵ (deg) ^f
1	6	L-LA	70	24	0.27	21	3000	3100	3200	1.05	155	−146
2	6	L-LA	70	48	0.62	48	6900	6800	7300	1.08	160	−147
3	6	L-LA	70	72	0.94	73	10 500	10 000	11 500	1.15	158	−147
4	6	L-LA	70	96	1.20	93	13 400	12 600	15 000	1.19	160	−146
5	6	L-LA	bulk	0.75	0.90	70	10 000	7500	10 500	1.40	148	
6	3	<i>rac</i> -LA	70	48	0.14	11	1500	3200	3400	1.05	120	
7	3	<i>rac</i> -LA	70	72	0.41	31	4400	5900	6500	1.09	121	
8	6	<i>rac</i> -LA	70	48	0.20	16	2300	3200	3500	1.08	121	
9	6	<i>rac</i> -LA	70	72	0.54	42	6000	6800	7500	1.09	122	
10	6	<i>rac</i> -LA	bulk	0.75	0.79	61	8700	6600	9500	1.44	115	
11	6	<i>rac</i> -LA ^g	70	48	0.69	54	7700	6600	7500	1.13	119	

^a Polymerization conditions: 90 μ mol of initiator; [L-lactide]₀/[**6**]₀ = 100 and [*rac*-LA]₀/[initiator]₀ = 100, in toluene. ^b Percentage conversion of the monomer (weight monomer/weight of polymer recovered \times 100). ^c Theoretical *M*_n = (monomer/initiator) \times (% conversion) \times (*M*_w of lactide). ^d Determined by GPC relative to polystyrene standards in tetrahydrofuran. ^e PLA melting temperature. ^f Optical rotation data of poly(L-lactide) obtained. [α]_D²⁵ values of L-lactide and poly(L-lactide) are −285° and −144°, respectively.^{9b} ^g Addition of ^{*i*}PrOH to the precatalyst in a ratio of 1:1.

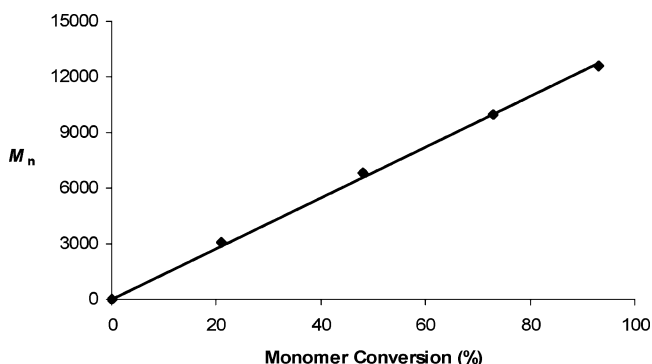


Figure 3. Plot of PLA *M*_n as a function of monomer conversion (%) for the polymerization of L-LA initiated by **6**; [L-LA]₀/[**6**]₀ = 100, toluene, 70 °C.

molecular weight distributions and linear correlations between *M*_n and percentage conversion (Figure 3). These results are characteristic of well-controlled living propagations as well as the existence of a single type of reaction site.

PLA end-group analysis by ¹H NMR spectroscopy showed that, as for the preparation of PCL, the polymerization was initiated by nucleophilic attack of the alkyl group on lactide.

Complexes **3** and **6** were also tested for the polymerization of *rac*-lactide, an equimolar mixture of the D- and L-lactide, in toluene at 70 °C (Table 3, entries 6–11). Derivative **3** gave 11% conversion of 100 equiv after 48 h (entry 6) and produced low molecular weight material with very narrow polydispersity (*M*_w = 3 400, *M*_w/*M*_n = 1.05). When the reaction was extended to 72 h the activity increased, with conversion rising to 31% without a significant increase in polydispersity (*M*_w/*M*_n = 1.09, entry 7). Complex **6** showed higher productivity, and, after 72 h, 42% of the monomer was converted with a very narrow

molecular weight distribution (*M*_w/*M*_n = 1.09, entry 9), while under bulk conditions 61% of the polymer was recovered after 45 min, with broader polydispersity (*M*_w/*M*_n = 1.44, entry 10). We attribute the broad molecular weight distribution to slow initiation (relative to propagation) of the initiator and gradual catalyst decomposition. In all cases (entries 6–11), low melting materials were obtained (*T*_m \approx 120 °C). Although very few group 2 alkyl initiators²² have been shown to act as active single-site catalysts for the ROP of *rac*-lactide, excellent tris(pyrazolyl)-hydroborate-based alkoxide magnesium complexes have previously been reported^{9b} to produce poly(lactides) with high stereocontrol in the polymer microstructures as well as narrow molecular weight distributions. Accordingly, we decided to transform “in situ” the alkyl group into an isopropoxide group that would be a more suitable mimic of the putative propagating alkoxide species. In a result consistent with this assumption, addition of 1 equiv of HO^{*i*}Pr to the precatalyst **6** led to a significant increase in activity, with the conversion rising from 16% to 54% with a slightly broader molecular weight distribution (entry 11, *M*_w/*M*_n = 1.13) obtained under otherwise identical conditions. The polymer characteristics were unchanged.

Microstructural analysis of the poly(*rac*-lactide) by ¹H NMR spectroscopy revealed that **3** exerts a low degree of stereoselectivity. This conclusion is based on the fact that the heterotactic tetrads **isi** and **sis** were not greatly enhanced as a result of the preference of the consecutive alternate insertion of the L- and D-lactide units into the growing chain. This behavior during the propagation is most probably the result of the low steric demand of the methyl substituents in the two pyrazole rings. This leads to sterically less congested and more flexible (and therefore less selective) active centers, even in the permanent presence of the sterically hindered ^{*t*}Bu amidinate substituent in the position *cis* to the alkyl leaving group.

These results are similar to previous observations made by Chisholm and Bochmann on magnesium alkoxides [(BDI)Mg-(O^tBu)(THF)],²⁶ [(η^3 -trispyrazolylborate)MgOR],^{9b} and magnesium alkyls [(BDI)Mg(η^1 -C₃H₅)(THF)],²² respectively, which polymerize *rac*-lactide to atactic poly(lactide). Rather interestingly, in the ¹³C{¹H} spectrum we did find some evidence for the formation of tetrad sequences usually derived from the polymerization of *meso*-lactide, a fact that could be due to a trans-esterification process in the polymer chain because polymerization of *L*-lactide shows only **iii** tetrads.

In conclusion, we report here a facile synthesis for a new family of alkyl magnesium complexes of the type [Mg(R)-(NNN)] (**1–6**) supported by a recently reported class of amidinate-based heteroscorpionate ligands. As observed in similar homoscorpionate systems, complexes **1–3**, **5**, and **6** undergo ligand redistribution, and the corresponding 6-coordinated sandwich complexes [Mg(tpamd)₂] (**7**) and [Mg(pbamd)₂] (**8**) are formed on heating to 90 °C in toluene. Interestingly, allyl derivative **4** can be easily transformed at room temperature. In addition, we obtained the cationic sandwich complex [Mg(tpamdH)₂]Cl₂ (**9**) by protonation of both acetamidinate moieties of the heteroscorpionate ligands and their transformations into acetamidine units. The alkyl ligands are sufficiently nucleophilic for attack on cyclic esters, so that the κ^3 -NNN alkyl magnesium complexes can act as single-site, living initiators for the well-controlled polymerization of polar monomers over a wide range of temperatures. ϵ -Caprolactone is polymerized within seconds to high molecular weight polymers with narrow polydispersities. Not surprisingly, the polymerization of LA occurs more slowly than that of CL but offers very good control. *L*-Lactide afforded highly crystalline, isotactic PLA materials with medium molecular weights, polydispersities as narrow as $M_w/M_n = 1.05$, and high melting temperatures ($T_m = 160$ °C). Propagation occurs without observable epimerization. *rac*-Lactide gave low levels of heterotactic PLA. Work is continuing in our laboratories to synthesize new group 2 initiators with much more sterically hindered heteroscorpionate ligands capable of inducing high levels of stereoselectivity and also to develop new polyester architectures.

Experimental Section

General Procedures. All manipulations were performed under nitrogen using standard Schlenk techniques. Solvents were predried over sodium wire (toluene, *n*-hexane, THF, diethyl ether) or calcium hydride (dichloromethane) and distilled under nitrogen from sodium (toluene), sodium–potassium alloy (*n*-hexane), sodium–benzophenone (THF, diethyl ether), or calcium hydride (dichloromethane). Deuterated solvents were stored over activated 4 Å molecular sieves and degassed by several freeze–thaw cycles. Microanalyses were carried out with a Perkin-Elmer 2400 CHN analyzer. ¹H and ¹³C NMR spectra were recorded on a Varian Mercury FT-400 spectrometer and referenced to the residual deuterated solvent. The NOESY-1D spectra were recorded on a Varian Inova FT-500 spectrometer with the following acquisition parameters: irradiation time 2 s and number of scans 256, using standard VARIAN-FT software. Two-dimensional NMR spectra were acquired using standard VARIAN-FT software and processed using an IPC-Sun computer. The Grignard reagents RMgCl were used as purchased (Aldrich). [Li(κ^3 -tpamd)(THF)] and [Li(κ^3 -pbamd)(THF)] were prepared according to literature procedures.¹⁷ ϵ -Caprolactone was dried by stirring over fresh CaH₂ for 48 h, then distilled under

reduced pressure and stored over activated 4 Å molecular sieves. *L*-Lactide and *rac*-lactide were sublimed twice, recrystallized from THF, and finally sublimed again prior to use. Gel permeation chromatography (GPC) measurements were performed on a Polymer Laboratories PL-GPC-220 instrument equipped with a PLgel 5 Å Mixes-C column, a refractive index detector, and a PD2040 light-scattering detector. The GPC column was eluted with THF at 40 °C at 1 mL/min and was calibrated using eight monodisperse polystyrene standards in the range 580–483 000 Da. PLA melting temperatures were measured using a melting point block (SMP 10). The sample was heated to 100 °C and then heated at a rate of 1 °C/min to 165 °C. The specific rotation [α]_D²² was measured at a concentration of 10 mg/mL in CHCl₃ at 22 °C on a Perkin-Elmer 241 polarimeter equipped with a sodium lamp operating at 589 nm with a light path length of 10 cm.

Preparation of Compounds 1–8. Synthesis of [Mg(C₃H₅)-(tpamd)] (1**).** In a 250 mL Schlenk tube, [Li(tpamd)(THF)] (1.00 g, 2.45 mmol) was dissolved in dry toluene (70 mL) and cooled to –70 °C. A 2.0 M THF solution of C₃H₅MgCl (1.22 mL, 2.45 mmol) was added, and the mixture was allowed to warm to room temperature and stirred during 1 h. The suspension was filtered, and the resulting yellow solution was concentrated to 20 mL. The solution was cooled to –26 °C, and this gave compound **1** as a pale yellow crystalline solid. Yield: 730 mg (1.85 mmol, 75%). Anal. Calcd for C₂₁H₃₄MgN₆: C, 63.88; H, 8.68; N, 21.28. Found: C, 63.92; H, 8.78; N, 21.32. ¹H NMR (C₆D₆, 297 K): δ 7.19 (s, 1H, CH), 7.04 (m, 1H, CH₂CHCH₂), 5.14 (s, 2H, H⁴), 3.55 (q, 2H, ³J_{H–H} = 6.8 Hz, CH₂–CH₃), 3.38 (d, 4H, ³J_{H–H} = 11.2 Hz, CH₂CHCH₂), 2.07 (s, 6H, Me⁵), 1.82 [s, 9H, C(CH₃)₃], 1.61 (s, 6H, Me³), 1.49 (t, 3H, ³J_{H–H} = 6.8 Hz, CH₂–CH₃). ¹³C{¹H} NMR (C₆D₆, 297 K): δ 153.7 (N=C–N), 150.0, 140.6 (C^{3or5}), 147.8 (CH₂CHCH₂), 106.3 (C⁴), 59.5 (CH₂CHCH₂), 59.2 (CH), 52.7 [C–(CH₃)₃], 44.2 (CH₂–CH₃), 31.0 [C(CH₃)₃], 19.6 (CH₂–CH₃), 13.1 (Me⁵), 10.4 (Me³).

Synthesis of [Mg(^tBu)(tpamd)] (2**).** In a 250 mL Schlenk tube, [Li(tpamd)(THF)] (1.00 g, 2.45 mmol) was dissolved in dry toluene (70 mL) and cooled to –70 °C. A 2.0 M THF solution of ^tBuMgCl (1.22 mL, 2.45 mmol) was added, and the mixture was allowed to warm to room temperature and stirred during 6 h. The suspension was filtered, and the resulting yellow solution was concentrated to 20 mL. The solution was cooled to –26 °C, and this gave compound **2** as a pale yellow crystalline solid. Yield: 798 mg (1.94 mmol, 79%). Anal. Calcd for C₂₂H₃₈MgN₆: C, 64.31; H, 9.32; N, 20.45. Found: C, 64.39; H, 9.39; N, 20.57. ¹H NMR (C₆D₆, 297 K): δ 7.19 (s, 1H, CH), 5.17 (s, 2H, H⁴), 3.55 (q, 2H, ³J_{H–H} = 7.0 Hz, CH₂–CH₃), 2.11 (s, 6H, Me⁵), 1.83 [s, 9H, N–C(CH₃)₃], 1.67 [s, 9H, Mg–C(CH₃)₃], 1.66 (s, 6H, Me³), 1.47 (t, 3H, ³J_{H–H} = 7.0 Hz, CH₂–CH₃). ¹³C{¹H} NMR (C₆D₆, 297 K): δ 153.9 (N=C–N), 150.0, 140.5 (C^{3or5}), 106.6 (C⁴), 59.4 (CH), 52.4 [N–C(CH₃)₃], 44.3 (CH₂–CH₃), 34.8 [Mg–C(CH₃)₃], 34.7 [Mg–C(CH₃)₃], 30.9 [N–C(CH₃)₃], 19.6 (CH₂–CH₃), 13.7 (Me⁵), 10.5 (Me³).

Synthesis of [Mg(CH₂SiMe₃)(tpamd)] (3**).** In a 250 mL Schlenk tube, [Li(tpamd)(THF)] (1.00 g, 2.45 mmol) was dissolved in dry toluene (70 mL) and cooled to –70 °C. A 1.0 M THF solution of CH₂SiMe₃MgCl (2.45 mL, 2.45 mmol) was added, and the mixture was allowed to warm to room temperature and stirred during 6 h. The suspension was filtered, and the resulting pale orange solution was concentrated to dryness. The residue was extracted with hexane (2 × 40 mL), and the resulting solution was concentrated to 20 mL. The solution was cooled to –26 °C, and this gave compound **3** as a pale orange crystalline solid. Yield: 840 mg (1.90 mmol, 77%). Anal. Calcd for C₂₂H₄₀MgN₆Si: C, 59.92; H, 9.14; N, 19.06. Found: C, 60.05; H, 9.22; N, 19.14. ¹H NMR (C₆D₆, 297 K): δ 7.18 (s, 1H, CH), 5.15 (s, 2H, H⁴), 3.56 (q, 2H, ³J_{H–H} = 7.0 Hz, CH₂–CH₃), 2.10 (s, 6H, Me³), 1.85 [s, 9H, C(CH₃)₃], 1.63 (s, 6H, Me⁵), 1.49 (t, 3H, ³J_{H–H} = 7.0 Hz,

(26) Chisholm, M. H.; Huffman, J. C.; Phomphrai, K. *J. Chem. Soc., Dalton Trans.* **2001**, 222.

Table 4. Crystal Data and Summary of Data Collection and Refinement Details for **1** and **9**

	1	9
formula	C ₂₁ H ₃₃ MgN ₆	C ₃₆ H ₆₀ Cl ₂ MgN ₁₂ ·4CDCl ₃
crystal size, mm	0.21 × 0.34 × 0.43	0.15 × 0.22 × 0.31
fw	393.84	1237.64
crystal class	monoclinic	monoclinic
space group	P2 ₁ /n	P2 ₁ /n
a, Å	12.001(4)	11.453(3)
b, Å	13.847(5)	14.319(3)
c, Å	14.450(5)	17.840(4)
α, deg	90	90
β, deg	113.049(5)	95.953(4)
γ, deg	90	90
V, Å ³	2210(1)	2910(1)
Z	4	2
D _{calcd} , Mg/m ³	1.184	1.408
μ, mm ⁻¹	0.099	0.714
F(000)	852	1276
no. of ind. reflections	1793 (R _{int} = 0.0424)	1549 (R _{int} = 0.0591)
no. observed reflections (I > 2σ _i)	1467	1168
data/restraints/parameters	1793/0/262	1549/0/374
GOF	0.532	0.741
final R indices (all data)	R ₁ = 0.0423, wR ₂ = 0.1212	R ₁ = 0.0506, wR ₂ = 0.1533
final R indices (obs. data)	R ₁ = 0.0527, wR ₂ = 0.1401	R ₁ = 0.0676, wR ₂ = 0.1795
location of largest diff. peak(s)	0.423, -0.412	0.541, -0.206

CH₂-CH₃), 0.52 [s, 9H, CH₂Si(CH₃)₃], -0.81 [s, 2H, CH₂Si(CH₃)₃]. ¹³C{¹H} NMR (C₆D₆, 297 K): δ 154.0 (N=C-N), 149.9, 140.4 (C^{3or5}), 106.3 (C⁴), 59.4 (CH), 52.7 [C(CH₃)₃], 44.2 (CH₂-CH₃), 31.5 [C(CH₃)₃], 19.6 (CH₂-CH₃), 13.4 (Me³), 10.4 (Me⁵), 5.1 [CH₂-Si(CH₃)₃], -7.1 [CH₂Si(CH₃)₃].

Synthesis of [Mg(C₃H₅)(pbpamd)] (4). In a 250 mL Schlenk tube, [Li(pbpamd)(THF)] (1.00 g, 2.45 mmol) was dissolved in dry toluene (70 mL) and cooled to -70 °C. A 2.0 M THF solution of C₃H₅MgCl (1.22 mL, 2.45 mmol) was added, and the mixture was allowed to warm to room temperature and stirred during 1 h. The suspension was filtered, and the resulting yellow solution was concentrated to 20 mL. The solution was cooled to -26 °C, and this gave compound **4** as a yellow crystalline solid. Yield: 725 mg (1.84 mmol, 75%). Anal. Calcd for C₂₁H₃₄MgN₆: C, 63.88; H, 8.68; N, 21.28. Found: C, 63.95; H, 8.79; N, 21.36. ¹H NMR (C₆D₆, 297 K): δ 7.31 (s, 1H, CH), 7.01 (m, 1H, CH₂CHCH₂), 5.18 (s, 2H, H⁴), 4.61 [m, 1H, ³J_{H-H} = 6.3 Hz, CH-(CH₃)₂], 3.80 [m, 1H, ³J_{H-H} = 5.9 Hz, CH-(CH₃)₂], 3.39 (d, 4H, ³J_{H-H} = 11.3 Hz, CH₂CHCH₂), 2.06 (s, 6H, Me⁵), 1.72 (s, 6H, Me³), 1.48 [d, 6H, ³J_{H-H} = 6.3 Hz, CH-(CH₃)₂], 1.33 [d, 6H, ³J_{H-H} = 5.9 Hz, CH-(CH₃)₂]. ¹³C{¹H} NMR (C₆D₆, 297 K): δ 152.2 (N=C-N), 150.0, 140.6 (C^{3or5}), 147.7 (CH₂CHCH₂), 106.0 (C⁴), 58.8 (CH₂CHCH₂), 58.1 (CH), 50.0 [CH-(CH₃)₂], 44.6 [CH-(CH₃)₂], 27.7 [CH-(CH₃)₂], 25.2 [CH-(CH₃)₂], 13.1 (Me⁵), 10.5 (Me³).

Synthesis of [Mg(Bu)(pbpamd)] (5). In a 250 mL Schlenk tube, [Li(pbpamd)(THF)] (1.00 g, 2.45 mmol) was dissolved in dry toluene (70 mL) and cooled to -70 °C. A 2.0 M THF solution of ^tBuMgCl (1.22 mL, 2.45 mmol) was added, and the mixture was allowed to warm to room temperature and stirred during 6 h. The suspension was filtered, and the resulting yellow solution was concentrated to 20 mL. The solution was cooled to -26 °C, and this gave compound **5** as a pale yellow crystalline solid. Yield: 810 mg (1.97 mmol, 80%). Anal. Calcd for C₂₂H₃₈MgN₆: C, 64.31; H, 9.32; N, 20.45. Found: C, 64.36; H, 9.35; N, 20.52. ¹H NMR (C₆D₆, 297 K): δ 7.33 (s, 1H, CH), 5.19 (s, 2H, H⁴), 4.68 [m, 1H, ³J_{H-H} = 6.3 Hz, CH-(CH₃)₂], 3.81 [m, 1H, ³J_{H-H} = 5.9 Hz, CH-(CH₃)₂], 2.10 (s, 6H, Me⁵), 1.76 (s, 6H, Me³), 1.70 [s, 9H, C(CH₃)₃], 1.48 [d, 6H, ³J_{H-H} = 6.3 Hz, CH-(CH₃)₂], 1.32 [d, 6H, ³J_{H-H} = 5.9 Hz, CH-(CH₃)₂]. ¹³C{¹H} NMR (C₆D₆, 297 K): δ 152.5 (N=C-N), 149.9, 140.5 (C^{3or5}), 106.5 (C⁴), 58.1 (CH), 50.0 [CH-(CH₃)₂], 44.5 [CH-(CH₃)₂], 35.1 [C(CH₃)₃], 34.9 [C(CH₃)₃], 27.7 [CH-(CH₃)₂], 25.1 [CH-(CH₃)₂], 13.6 (Me⁵), 10.6 (Me³).

Synthesis of [Mg(CH₂SiMe₃)(pbpamd)] (6). In a 250 mL Schlenk tube, [Li(pbpamd)(THF)] (1.00 g, 2.45 mmol) was dissolved in dry toluene (70 mL) and cooled to -70 °C. A 1.0 M THF solution of Me₃SiCH₂MgCl (2.45 mL, 2.45 mmol) was added, and the mixture was allowed to warm to room temperature and stirred during 6 h. The suspension was filtered, and the resulting pale orange solution was concentrated to dryness. The residue was extracted with hexane (2 × 40 mL), and the resulting solution was concentrated to 20 mL. The solution was cooled to -26 °C, and this gave compound **6** as a pale orange crystalline solid. Yield: 815 mg (1.85 mmol, 75%). Anal. Calcd for C₂₂H₄₀MgN₆Si: C, 59.92; H, 9.14; N, 19.06. Found: C, 60.00; H, 9.19; N, 19.12. ¹H NMR (C₆D₆, 297 K): δ 7.32 (s, 1H, CH), 5.18 (s, 2H, H⁴), 4.67 [m, 1H, ³J_{H-H} = 6.6 Hz, CH-(CH₃)₂], 3.80 [m, 1H, ³J_{H-H} = 5.9 Hz, CH-(CH₃)₂], 2.09 (s, 6H, Me³), 1.71 (s, 6H, Me⁵), 1.51 [d, 6H, ³J_{H-H} = 6.6 Hz, CH-(CH₃)₂], 1.34 [d, 6H, ³J_{H-H} = 5.9 Hz, CH-(CH₃)₂], 0.52 [s, 9H, CH₂Si(CH₃)₃], -0.78 [s, 2H, CH₂Si(CH₃)₃]. ¹³C{¹H} NMR (C₆D₆, 297 K): δ 152.4 (N=C-N), 149.8, 140.4 (C^{3or5}), 106.3 (C⁴), 58.1 (CH), 50.0 [CH-(CH₃)₂], 44.7 [CH-(CH₃)₂], 27.7 [CH-(CH₃)₂], 25.5 [CH-(CH₃)₂], 13.4 (Me³), 10.5 (Me⁵), 5.1 [CH₂Si(CH₃)₃], -8.1 [CH₂Si(CH₃)₃].

Synthesis of [Mg(tbpamd)] (7). In a 250 mL Schlenk tube, [Mg(C₃H₅)(tbpamd)] (**1**) (1.00 g, 2.53 mmol) or [Mg(^tBu)(tbpamd)] (**2**) (1.00 g, 2.43 mmol) or [Mg(CH₂SiMe₃)(tbpamd)] (**3**) (1.00 g, 2.27 mmol) was dissolved in dry toluene (70 mL), and the solution was heated at 90 °C and stirred during 96 h. The resulting yellow solution was concentrated to 20 mL. The solution was cooled to -26 °C, and this gave compound **7** as a white crystalline solid. Yield: from **1** = 710 mg (1.04 mmol, 82%), from **2** = 720 mg (1.05 mmol, 86%), from **3** = 680 mg (0.99 mmol, 87%). Anal. Calcd for C₃₆H₅₈MgN₁₂: C, 63.29; H, 8.56; N, 24.60. Found: C, 63.36; H, 8.64; N, 24.68. **7a** ¹H NMR (C₆D₆, 297 K): δ 7.06 (s, 2H, CH), 5.53 (s, 4H, H⁴), 3.18 (q, 4H, ³J_{H-H} = 6.6 Hz, CH₂-CH₃), 2.22 (s, 12H, Me³), 1.89 (s, 12H, Me⁵), 1.53 [s, 18H, C(CH₃)₃], 1.43 (t, 6H, ³J_{H-H} = 6.6 Hz, CH₂-CH₃). ¹³C{¹H} NMR (C₆D₆, 297 K): δ 154.5 (N=C-N), 150.4, 141.8 (C^{3or5}), 106.4 (C⁴), 59.5 (CH), 50.9 [C(CH₃)₃], 44.3 (CH₂-CH₃), 35.0 [C(CH₃)₃], 19.3 (CH₂-CH₃), 13.5 (Me³), 11.3 (Me⁵). **7b** ¹H NMR (C₆D₆, 297 K): δ 7.11 (s, 2H, CH), 5.43 (s, 2H, H⁴), 5.41 (s, 2H, H⁴), 4.08 (m, 2H, CH₂-CH₃), 3.61 (m, 2H, CH₂-CH₃), 2.20 (s, 6H, Me³), 1.94 (s, 6H, Me³), 1.92 (s, 6H, Me⁵), 1.67 (m, 6H, CH₂-CH₃), 1.59 [s, 18H, C(CH₃)₃], 1.53 (s, 6H, Me⁵). ¹³C{¹H} NMR (C₆D₆, 297 K): δ 154.6 (N=C-N), 152.1, 150.0, 142.0, 139.9 (C^{3or5}),

106.6, 105.5 (C⁴), 59.9 (CH), 51.0 [C(CH₃)₃], 44.2, 42.4 (CH₂-CH₃), 34.7 [C(CH₃)₃], 19.8 (CH₂-CH₃), 14.1, 11.9 (Me³), 11.5, 10.6 (Me⁵).

Synthesis of [Mg(pbpamd)]₂ (8). In a 250 mL Schlenk tube, [Mg(C₃H₅)(pbpamd)] (**4**) (1.00 g 2.53 mmol) or [Mg(^tBu)(pbpamd)] (**5**) (1.00 g, 2.43 mmol) or [Mg(CH₂SiMe₃)(pbpamd)] (**6**) (1.00 g, 2.27 mmol) was dissolved in dry toluene (70 mL), and the solution was stirred at room temperature during 2 h for compound **4** or heated at 90 °C and stirred during 96 h for compounds **5** and **6**. The resulting yellow solution was concentrated to 20 mL. The solution was cooled to -26 °C, and this gave compound **8** as a white crystalline solid. Yield: from **4** = 740 mg (1.08 mmol, 86%), from **5** = 710 mg (1.04 mmol, 85%), from **6** = 670 mg (0.98 mmol, 86%). Anal. Calcd for C₃₆H₅₈MgN₁₂: C, 63.29; H, 8.56; N, 24.60. Found: C, 63.34; H, 8.62; N, 24.65. ¹H NMR (C₆D₆, 297 K): δ 7.41 (s, 2H, CH), 5.43 (s, 2H, H⁴), 5.39 (s, 2H, H⁴), 4.74 [m, 2H, CH-(CH₃)₂], 3.93 [m, 2H, CH-(CH₃)₂], 2.14 (s, 6H, Me³), 1.86 (s, 6H, Me³), 1.84 (s, 6H, Me⁵), 1.66 (d, 6H, ³J_{H-H} = 6.6 Hz, CH-(CH₃)₂), 1.58 [d, 6H, ³J_{H-H} = 5.9 Hz, CH-(CH₃)₂], 1.50 [d, 6H, ³J_{H-H} = 5.9 Hz, CH-(CH₃)₂], 1.29 [d, 6H, ³J_{H-H} = 5.9 Hz, CH-(CH₃)₂], 1.18 (s, 6H, Me⁵). ¹³C{¹H} NMR (C₆D₆, 297 K): δ 153.9 (N=C-N), 150.5, 148.7, 139.0, 138.4 (C^{3or5}), 106.3, 105.7 (C⁴), 59.4 (CH), 49.8, 47.1 [CH-(CH₃)₂], 27.8, 27.7, 23.9, 23.1 [CH-(CH₃)₂], 14.1, 12.0 (Me³), 10.8, 10.2 (Me⁵).

Synthesis of [Mg(tbpamdH)₂]Cl₂ (9). In a 250 mL Schlenk tube, [Mg(tbpamd)]₂ (**7**) (1.00 g, 1.46 mmol) was dissolved in dry THF (70 mL). A 2.0 M solution of HCl in Et₂O (1.46 mL, 2.92 mmol) was added, and the mixture was stirred overnight. The solvent was removed in vacuo to give a white solid, which was washed with hexane (40 mL) and identified as **9**. Yield: 950 mg (1.26 mmol, 90%). Anal. Calcd for C₃₆H₆₀Cl₂MgN₁₂: C, 57.18; H, 8.00; N, 22.23. Found: C, 57.25; H, 8.06; N, 22.29. ¹H NMR (CDCl₃, 297 K): δ 7.71 (s, 2H, NH), 7.21 (s, 2H, CH), 5.94 (s, 4H, H⁴), 3.80 (q, 4H, ³J_{H-H} = 7.0 Hz, CH₂-CH₃), 2.73 (s, 12H, Me³), 2.58 (s, 12H, Me⁵), 1.49 [s, 18H, C(CH₃)₃], 1.16 (t, 6H, ³J_{H-H} = 7.0 Hz, CH₂-CH₃). ¹³C{¹H} NMR (C₆D₆, 297 K): δ 159.8 (N=C-N), 152.6, 143.3 (C^{3or5}), 107.8 (C⁴), 65.4 (CH), 54.5 [C(CH₃)₃], 42.5 (CH₂-CH₃), 31.6 [C(CH₃)₃], 17.3 (CH₂-CH₃), 13.8 (Me⁵), 12.3 (Me³).

X-ray Crystallographic Structure Determination for Complexes 1 and 9. A summary of crystal data collection and refinement parameters for compounds **1** and **9** is given in Table 4.

Single crystals of **1** and **9** were mounted on a glass fiber and transferred to a Bruker X8 APEX II CCD-based diffractometer equipped with a graphite monochromated Mo K α radiation source ($\lambda = 0.71073$ Å). Data were integrated using SAINT,²⁷ and an absorption correction was performed with the program SADABS.²⁸ The software package SHELXTL version 6.12²⁹ was used for space

group determination, structure solution, and refinement by full-matrix least-squares methods based on F^2 . All non-hydrogen atoms were refined with anisotropic thermal parameters. Hydrogen atoms were placed using a "riding model" and included in the refinement at calculated positions.

Polymerization Procedures. Polymerizations of ϵ -caprolactone (CL) were carried out on a Schlenk line in a flame-dried round-bottomed flask equipped with a magnetic stirrer. In a typical procedure, the initiator was dissolved in the appropriate amount of solvent, and the temperature equilibration was ensured by stirring the solution for 15 min on a temperature bath. ϵ -CL was injected, and polymerization times were measured from that point. Polymerizations were completed by addition of acetic acid (5 vol %) in methanol. Polymers were precipitated in methanol, filtered, dissolved in THF, reprecipitated in methanol, and dried in vacuo to constant weight.

Polymerizations of L-lactide and *rac*-lactide (LA) were performed on a Schlenk line in a flame-dried round-bottomed flask equipped with a magnetic stirrer. The Schlenk tubes were charged in the glovebox with the required amount of *rac*-lactide and initiator, separately, and then attached to the vacuum line. The initiator and monomer were dissolved in the appropriate amount of solvent, and the temperature equilibration was ensured in both Schlenk flasks by stirring the solution for 15 min in a bath. The appropriate amount of initiator was added by syringe, and polymerization times were measured from that point. Polymerizations were stopped by injecting a solution of acetic acid (5 vol %) in methanol. Polymers were precipitated in methanol, filtered, dissolved in THF, reprecipitated in methanol, and dried in vacuo to constant weight.

Acknowledgment. We gratefully acknowledge financial support from the Ministerio de Educación y Ciencia (Dirección General de Investigación), Spain (Grant No. CTQ 2005-07918-CO2-01-02), Consejería de Educación, Comunidad de Madrid, Spain (Grant No. S-0505/PPQ/0328), and Consejería de Educación y Ciencia, Comunidad de Castilla-La Mancha, Spain (Grant No. PBI05-023).

Supporting Information Available: Full crystallographic data for **1** and **9**. Figures giving additional NMR spectra. This material is available free of charge via the Internet at <http://pubs.acs.org>.

OM7007327

(27) SAINT+ v7.12a. Area-Detector Integration Program; Bruker-Nonius AXS: Madison, WI, 2004.

(28) Sheldrick, G. M. SADABS version 2004/1. A Program for Empirical Absorption Correction; University of Göttingen: Göttingen, Germany, 2004.

(29) SHELXTL-NT version 6.12. Structure Determination Package; Bruker-Nonius AXS: Madison, WI, 2001.